

PAPER • OPEN ACCESS

## Numerical modelling of velocity profile parameters of the atmospheric boundary layer simulated in wind tunnels

To cite this article: A Abubaker *et al* 2018 *IOP Conf. Ser.: Mater. Sci. Eng.* **393** 012025

View the [article online](#) for updates and enhancements.

You may also like

- [The Spatial Variation of Aerodynamic Parameters and Wind Erosion Potential in Southwestern Tarim Basin from Shifting Desert to Oasis](#)  
Jie Zhou, ShengYu Li, Xin Gao et al.
- [Assessment of Aerodynamic Roughness Length Using Remotely Sensed Land Cover Features and MODIS](#)  
Malik Rashid Abbas, Abd Wahid Bin Rasib, Talib Rashid Abbas et al.
- [Surface wind observations affected by agricultural development over Northwest China](#)  
Songjun Han, Qiuhong Tang, Xuezheng Zhang et al.



**ECS**  
The  
Electrochemical  
Society  
Advancing solid state &  
electrochemical science & technology

**DISCOVER**  
how sustainability  
intersects with  
electrochemistry & solid  
state science research

# Numerical modelling of velocity profile parameters of the atmospheric boundary layer simulated in wind tunnels

A Abubaker<sup>1</sup>, I Kostić<sup>1</sup> and O Kostić<sup>1</sup>

<sup>1</sup>University of Belgrade, Faculty of Mechanical Engineering, Aeronautical Department, Kraljice Marije 16, 11120 Belgrade 35, Serbia

E-mail: ikostic@mas.bg.ac.rs

**Abstract.** Experimental and numerical modeling and simulations of the wind influence within the atmospheric boundary layer are essential tools in optimum building structural design. Each of these methods, however, has both advantages and disadvantages. In experimental investigations performed in wind tunnels, reliable results can be obtained, but detailed information of the wind profile parameters, such as the surface roughness length  $z_0$  or the friction velocity  $u_*$ , are difficult to determine. Numerical simulations, on other hand, easily yield any information of the wind velocity profile. However, the reliability of numerical results strongly depends on the established and adopted computational model. This paper presents the computational fluid dynamics (CFD) analysis of the atmospheric boundary layer simulated in subsonic wind tunnels using appropriate types of obstacles, based on the *SST  $k-\omega$*  turbulence model with optimized unstructured mesh and optimum selection of relevant physical model parameters, performed in Ansys Fluent software. Results have been compared with the measurements from the Assiut University wind tunnel with maximum velocity of 4 m/s, and from subsonic wind tunnel at Belgrade University, with maximum air velocity of 45 m/s. Detailed comparisons for velocity distributions with these experimental results have shown very good conformity. Also, the three-parameter fitting methods were successfully established to define surface roughness length  $z_0$  and the friction velocity  $u_*$ . Obtained results have shown that the established numerical model is able to substitute a remarkable number of expensive wind tunnel tests hours within the operational investigations of wind influence on the building structures.

## 1. Introduction

The wind flow over different terrains has been investigated for many years in full scale measurements, numerical simulations and wind tunnel experiments. It is of great importance in many engineering areas, as for example pollution control, wind turbine sitting and large civil engineering constructions. Despite the use of numerical methods in the estimation of wind flow in different terrains, the results of those simulations as every other numerical model need to be verified in real physical experience [1].

Wind tunnels are generally classified into four groups according to flow speed. They are: subsonic or low-speed, transonic, supersonic, and hypersonic. Subsonic or low-speed wind tunnels are the most common type used in many applications. Atmospheric boundary layer wind tunnels (ABLWTs) are usually of the subsonic or low-speed type. Transonic wind tunnels are common in the aircraft industry since. Supersonic wind tunnels can be used to investigate the behavior of jet engines and military aircrafts. Hypersonic wind tunnels find their applications in rockets and space vehicles. A further way to categorize low speed wind tunnels is by dividing them into open loop or closed loop wind tunnels [2].



Content from this work may be used under the terms of the [Creative Commons Attribution 3.0 licence](https://creativecommons.org/licenses/by/3.0/). Any further distribution of this work must maintain attribution to the author(s) and the title of the work, journal citation and DOI.

The computational fluid dynamics (CFD) is a tool which has increasingly been used to study a wide variety of processes in the atmospheric boundary layer (ABL). There are several numerical models that can be employed in the simulation of the ABL due to their availability of appropriate boundary conditions and meteorological data [3, 4]. One of them is a shear stress transport (*SST*)  $k-\omega$  model which employs the  $k-\omega$  model near the surface, and  $k-\epsilon$  model in free flow. Good performance of the *SST*  $k-\omega$  model for ABL flow around blunt bodies has been shown, for example, in [5, 6].

This paper presents the computational fluid dynamics (CFD) analysis of the atmospheric boundary layer, simulated in wind tunnels. CFD results have been compared with the available experimental data from two subsonic wind tunnels, the Assiut University wind tunnel with maximum velocity of 4 m/s [7], and the Belgrade University (Faculty of Mechanical Engineering) wind tunnel, with maximum air velocity of 45 m/s [8]. Experimental data and CFD analyses have been used to estimate the mean velocity profiles in wind tunnel test sections for different flow speeds passed a variety of different obstacles, roughness elements and other devices, in order to validate the applied methodology for proper simulation of complex terrain influence on the ABL.

Also, mean velocity profiles in the surface layer can be characterized by determining the zero-plane displacement  $d$ , the roughness length  $z_0$  for the given roughness and boundary layer height. Accurate evaluation of these parameters requires knowledge of the shear velocity  $u_*$ , which may be measured directly using a skin-friction balance, inferred from Reynolds stress measurements, deduced using the momentum integral equation, or evaluated indirectly from the mean velocity profile [9, 10, 11, 12]. The indirect procedures are less time consuming, and they have been used for the analyses presented in this paper.

## 2. Wind velocity profiles in atmospheric boundary layer

There are two main methods for describing the mean horizontal wind profile in the ABL [13], the logarithmic, or log law and the power law (see Figure 1).

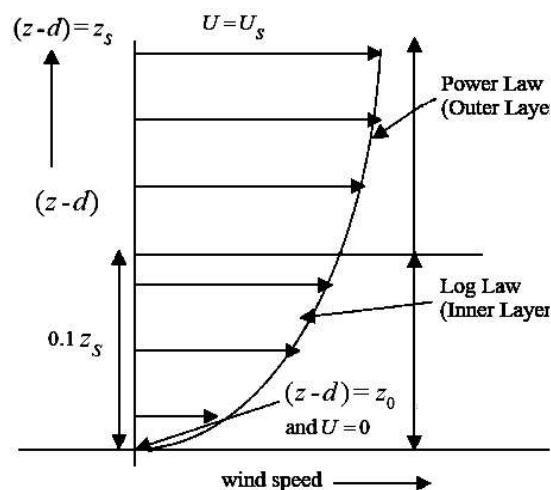


**Figure 1.** Log-law and power-law region in mean wind speed profile.

### 2.1. The log law model

According to the log law model, which is applied for inner ABL domain, the mean wind speed  $U(z)$  at height  $z$  above the ground can be mathematically expressed as:

$$U(z) = \frac{u_*}{k} \ln\left(\frac{z-d}{z_0}\right) \quad (1)$$

It can be rearranged as:

$$z = z_0 \exp\left(\frac{k U(z)}{u_*}\right) + d \quad (2)$$

where  $u_*$  is shear velocity,  $k$  is Von Karman's constant whose typical value is 0.4,  $d$  is zero-plane displacement which is the depth of still air trapped among the roughness elements, and  $z_0$  is roughness length which represents the size of the eddies produced from the wind moving over a rough surface.

Table 1 gives the appropriate value of roughness length, for various types of terrain types (adapted from the Australian Standard for Wind Loads, AS1170.2, 1989) [14].

**Table 1.** Terrain types, roughness length

Terrain types	roughness length (m)
Very flat terrain (snow, desert)	0.001-0.005
Open terrain (grassland, few trees)	0.01-0.05
Suburban terrain (buildings 3-5 m)	0.1-0.5
Dense urban (buildings 10-30 m)	1-5

### 2.2. The power law model

According to the power law, which is applied for outer ABL domain, the mean wind speed  $U(z)$  at height  $z$  above the ground can be expressed by equation:

$$U(z) = U_s \left(\frac{z-d}{z_s}\right)^\alpha \quad (3)$$

where  $U_s$  is the mean wind speed at a chosen reference height,  $z_s$  is the reference ABL height,  $\alpha$  is power index or exponent which changes with surface roughness (terrain type).

Figure 2 shows an example of different power law profiles (and corresponding  $\alpha$  values) for different types of terrain, obtained in [15].

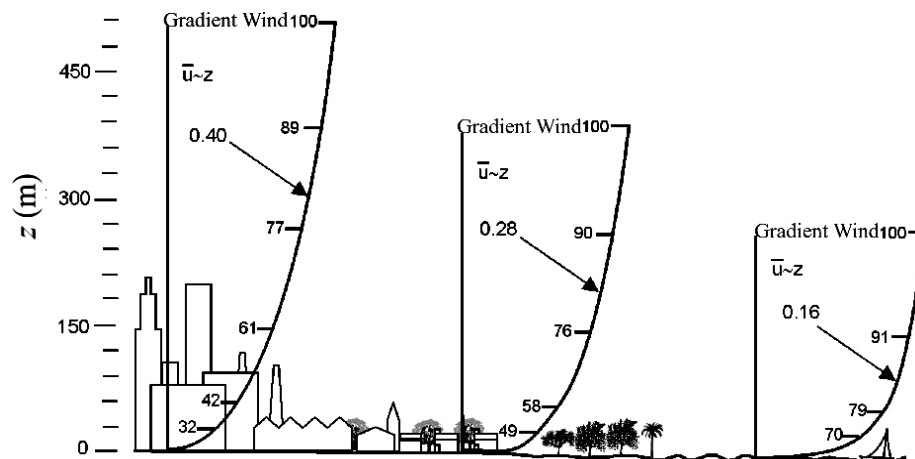


**Figure 2.** The power law profiles for the velocity distributions in boundary layer over different terrains.

### 3. Experimental facilities

Simulation of the ABL in a wind tunnel requires designing and experimenting with the different passive device configurations to be added at the entrance of the test section in order to create the desired boundary layer properties upstream of the test object (building, bridge, etc.). In this study, two wind tunnels have been chosen, and their experiments aimed to simulate the atmospheric boundary layer within the test section, at quite different flow speeds, have been presented.

First experiments were carried out in an open-loop, low-speed (up to 4 m/s), atmospheric boundary layer wind at the Mechanical Engineering Department of the Assiut University, as described in [7]. This wind tunnel had the test section with length of 1.7 m, and had 1×1 m square cross section area. The simulated ABL was generated along the 3.5 m boundary layer development section, by the use of three triangular flat spires combined with 710 cubes (roughness elements), as shown in Figure 3.



**Figure 3.** Photograph of the test section at the Assiut University wind tunnel.

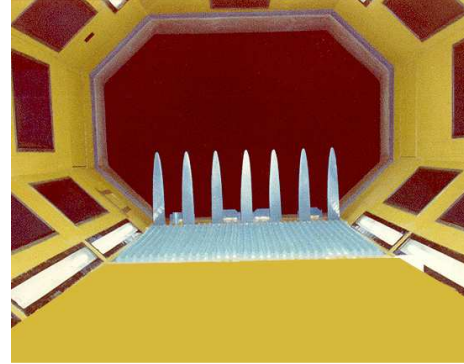


**Figure 4.** Photograph of the test section at the Belgrade University wind tunnel.

Mean vertical velocity distribution was measured at different heights in the middle of test section, at the distance 3.6 m from the inlet of the boundary layer development section, and experimental results have been obtained in the empty wind tunnel, wind tunnel with spires only, and wind tunnel with the combination of spires and arrays of roughness elements.

Second experiment was carried out in the wind tunnel built at the Belgrade University, Faculty of Mechanical Engineering (Aeronautical Engineering Department), which is of a closed-loop type. Its test section is 6 m long, with 2.8×2.2 m octagonal cross section, and maximum speed was up to 60 m/s with empty test section, at the time when tests were performed (more details described in [8]).

As shown in Figure 4, ABL was simulated by four small wall barriers, seven elliptic spires and 1156 small pyramids (roughness elements) placed on the floor, in the front domain of the test section. Mean velocity distribution was measured at 3 m distance from the test section inlet, at different heights from the floor.

#### 4. Calculation procedure

The CFD simulations, presented in this paper, were performed in ANSYS Fluent using 3D steady state, density-based, RANS approach with the *SST k- $\omega$*  model which was adopted by [16]. Fluid was air, and its viscosity was described by Sutherland law, using three coefficient method. Second order discretization schemes were used for the convective and viscous terms of the governing equations. Numerical convergence was achieved when the solution monitor for mass flow rate through the control volume outlet showed no change, and remained constant observing significant number of digits.

Due to the vertical symmetry of the flow, for both wind tunnels the half-models for the effuser and test section were modeled, in order to minimize the number of mesh elements within the control volume. The unstructured meshes were used for both cases, and attention was paid to appropriately increase the number of elements on the lower wall of test sections, but still keep the total number of elements at reasonably low values, with satisfactory mesh quality, see Figures 5 and 6.

Numerical analyses were applied for two cases for Assiut University wind tunnel - in the first case spires only were mounted on the lower wall of boundary layer development section, and in the second case both spires and surface roughness elements were used to simulate obstacles which generate atmospheric boundary layer. In Belgrade University wind tunnel, tests were performed with all elements included (wall barriers, spires and roughness elements mounted on the lower wall of test section).

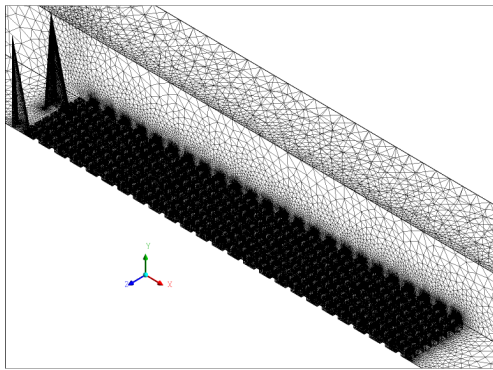


**Figure 5.** Unstructured surfaces mesh for the calculation of airflow at Assuit University.

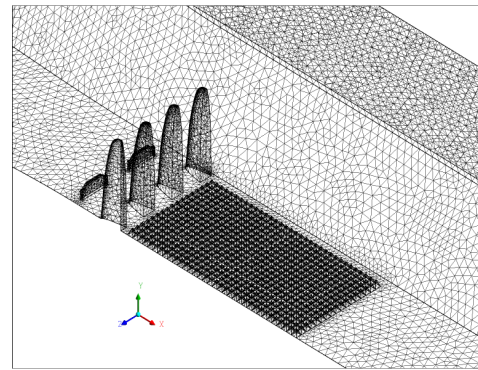


**Figure 6.** Unstructured surfaces mesh for the calculation of airflow at Belgrade University.

Also, the indirect methods used to estimate  $u^*$ ,  $z_0$  and  $d$  based either on experimental data, or numerical simulation, can be classified into several ways. One of the approaches uses the generalized reduced gradient (GRG) non-linear least squares method built in the Microsoft Office Excel Solver add-in [17], and it calculates the values of the three parameters  $u^*$ ,  $z_0$ , and  $d$  by minimizing the sum of squared differences between measured and predicted  $z$  values on the logarithmic law. The parameter values are selected from the results that best fit the considered velocity profile (the so-called three parameter fitting). The fitting procedure is also applied for the power law profiles.

## 5. Results and discussion

### 5.1. Comparison of CFD and wind tunnel results

All CFD simulations presented in this paper have been performed at 1:1 scale (i.e. using the actual wind tunnel model dimensions). The presentation of the CFD and wind tunnel results and their comparison has been done for three general cases, in order to validate here established computational method over a wide range of simulated wind speeds.

The first two cases consider the Assuit University wind tunnel tests and their CFD simulations. The flow velocities were obtained by three different fan speeds of 500, 1000, 1440 rpm during the tests, and the maximum flow speed achieved was 4 m/s at 1440 rpm.

Figure 7 shows comparisons between the numerically simulated and measured mean velocity profiles for different fan speeds, with only spires used for ABL generation. The CFD results and the

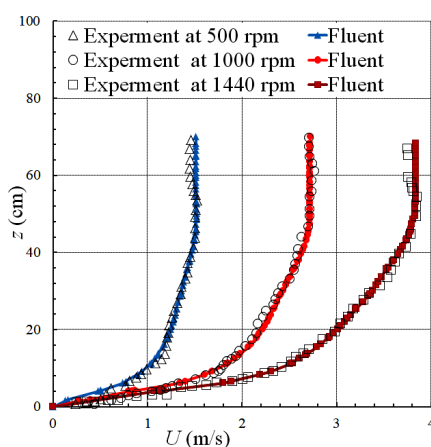


**Figure 7.** Mean velocity distribution comparisons for Assuit University wind tunnel, case with spires only.

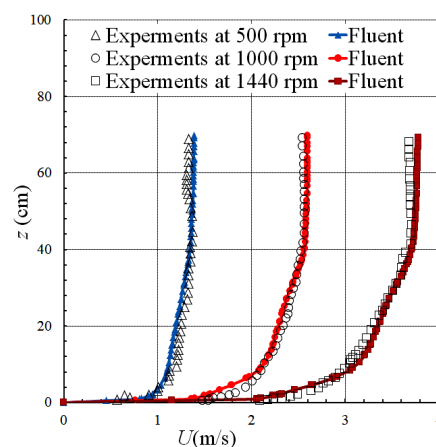


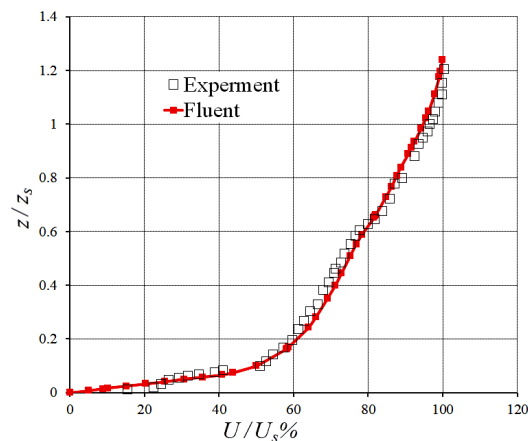
**Figure 8.** Mean velocity distribution comparisons for Assuit University wind tunnel, case of spires and roughness elements.

wind tunnel results are in fairly good agreement, except in the inner layer of ABL. In actual experiments, although no roughness elements were applied, the wind tunnel wall had its inherent surface roughness. Since this value was not published, the CFD calculations were performed assuming a smooth wall which, at such small speeds, has caused small inevitable differences between the measured and calculated speeds near the wall surface.

Figure 8 shows measured mean velocity profiles for different fan speeds compared with the CFD results. In this case, both spires and surface roughness elements were used, and comparison shows good agreements for velocity profiles across the whole relevant height.

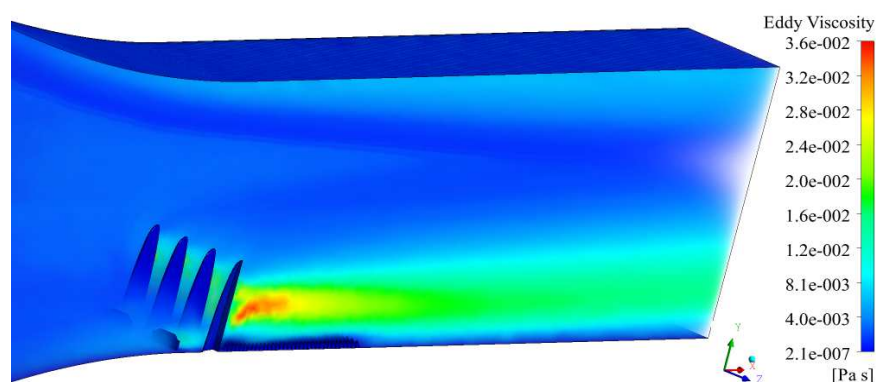
The third case considers the Belgrade University wind tunnel, where the experiment and here presented CFD calculations were performed for flow speed of 45 m/s, about ten times higher than the maximum flow speed achieved in the Assuit University wind tunnel. Relative velocity profiles  $U/U_0$  obtained along relative height  $z/z_s$  at the middle of test section are used for the presentation of both experimental and numerical results.

Figure 9 shows comparison between the experimental and the numerically obtained values of the relative velocity. The CFD results for this case also show good agreements with the experiment, for the practical engineering purposes.



**Figure 9.** Relative velocity profile comparisons for Belgrade University wind tunnel.

Figure 10 shows the spatial contour of eddy viscosity calculated for the Belgrade University wind tunnel test, the region of high eddy viscosity grows massively large behind the spires and then it fades out along the test section.



**Figure 10.** Eddy viscosity in Belgrade University wind tunnel.

5.2. Determination of wind velocity profile parameters

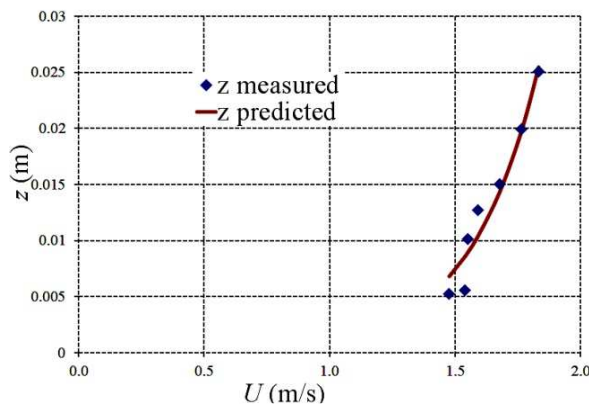
Indirect method used the validation of the logarithmic law in inner layer, from equation (2) predicted height  $z$  was plotted against measured height  $z$  at same value of measured velocity. Values of  $u^*$ ,  $z_0$  and  $d$  were determined from the height curve ( $z$ ) fitting, using the (GRG) non-linear least squares method.

Table 2 shows the estimated values of  $u^*$ ,  $z_0$  and  $d$  for three mentioned cases of atmospheric boundary layers simulations. The sum of squared residuals is computed and minimized using the Solver add-in to obtain the set of parameter values that best describes the experimental data. The confidence of best-fit values is then visualized and assessed in a generally applicable and easily comprehensible way.

**Table 2.** Values of  $u^*$ ,  $z_0$  and  $d$

	Shear velocity $u^*$ (m/s)	Roughness length $z_0$ (m)	Zero-plane displacement $d$ (m)
<b>Case 1</b> (Assuit, spire only)	0.108	0.0000285	0
<b>Case 2</b> (Assuit, spire and roughness)	0.239	0.0062	0
<b>Case 3</b> (Belgrade)	4.753	0.0101	0

Figures 11 and 12 show the best fits for cases 1 and 2, for the results from Assuit University wind tunnel, obtained at 1000 rpm fan speed. Figure 13 shows the fit for case 3, where the predicted height  $z$  values have been compared with the measured height  $z$  values taken from the experimental results from Belgrade University wind tunnel.



**Figure 11.** Best fit of predicted height  $z$  to measured height  $z$  for case 1.

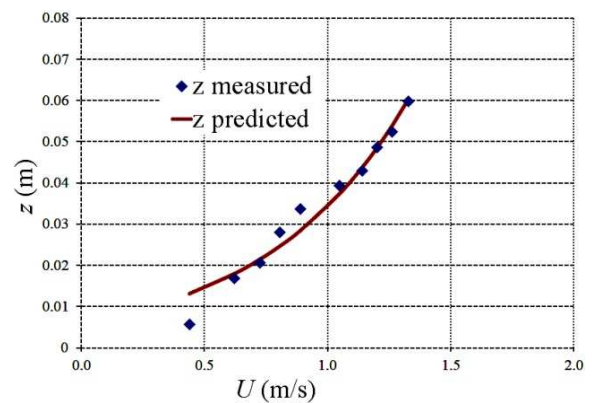


**Figure 12.** Best fit of predicted height  $z$  to measured height  $z$  for case 2.

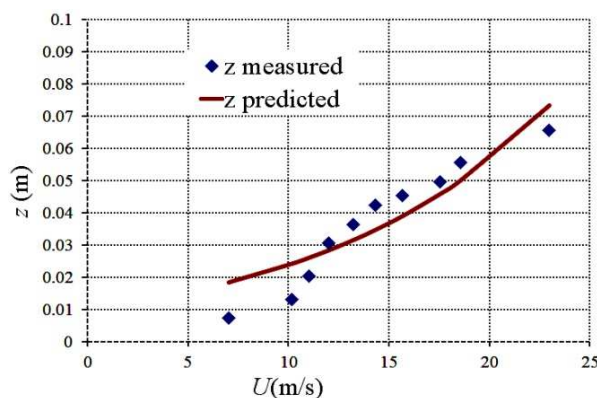


**Figure 13.** Best fit of predicted height  $z$  to measured height  $z$  for case 3.

Assuming an object model in scale 1:100 within the simulated ABL in wind tunnels, comparisons with Table 1 show that the estimated  $z_0$  for case 1 would correspond to very flat area (snow, desert), value  $z_0$  for case 2 would correspond to the urban and suburban area, while  $z_0$  for case 3 would correspond to the ABL generated by the dense urban area, with buildings 10-30 m. On the other hand, all determined zero-plane displacements are equal to zero, because measurements in wind tunnels were made downstream from the simulated surface roughnesses.

Also, the power law representation of the mean velocity profile in the outer ABL layer is possible and is often used in wind engineering applications. Values of  $\alpha$  were determined for power law expression in equation (3), after estimating the zero-plane displacement  $d$ .

Figures 14 and 15 show power law profiles for cases 1 and 2, compared with the measured relative velocity profiles from Assuit University wind tunnel, at 1000 rpm fan speed. For case 1, the power law gave computed value of  $\alpha = 0.12$ , corresponding to a flat area (also see figure 2), while for case 2 the computed value  $\alpha = 0.24$  would correspond to the suburban area.

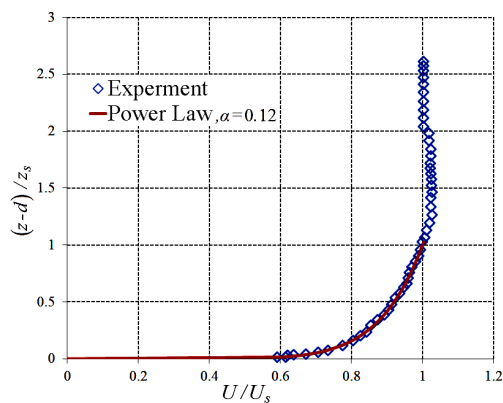


**Figure 14.** Best fit of the power law to measured relative velocity profile for case 1.

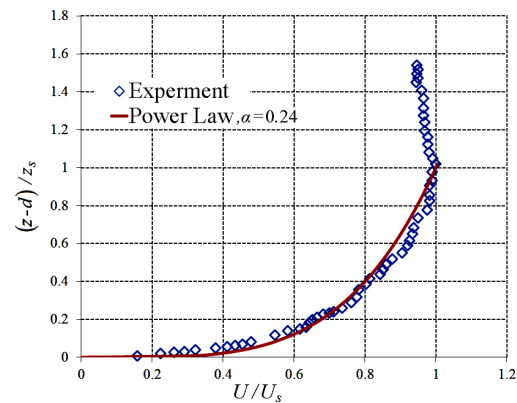


**Figure 15.** Best fit of the power law to measured relative velocity profile for case 2.

Figure 16 shows power law profile for case 3, i.e. the Belgrade University wind tunnel. Power law in this case gave the computed value of  $\alpha = 0.37$  which, compared with figure 2, would correspond to a large city area. These computations show that the obtained log law curves for the inner ABL layer, and power law dependences for the outer ABL layer, show very good match by categories. Namely, the first wind tunnel test case has obviously modeled the ABL that would correspond to a very smooth and flat area, the second would resemble boundary layer generated by a suburban domain, characterized by mixture of small houses and trees, while the third ABL would be generated by a big city building structures.

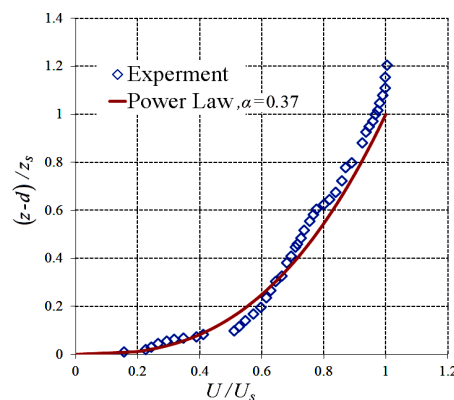


**Figure 16.** Best fit of the power law to measured relative velocity profile for case 3.

Previous section has shown that here presented CFD calculation model can readily be used as a “virtual” wind tunnel and substitute many hours of expensive real wind tunnel tests, spent in the preparations of optimum obstacle setups for ABL simulations, for wind velocities in the range from 1 to 45 m/s. In that case, the log and power law fitting methods shown in this section should also be used to verify if the wind tunnel obstacle setups, defined through the CFD modeling and analyses, would give the desired type of atmospheric boundary layer velocity profile. This is mandatory for proper testing of the wind influence on any desired building structure in its natural environment, either if we use the real, or here presented “virtual” CFD wind tunnel for that purpose.

## 6. Conclusion

The atmospheric boundary layer (ABL) is the region of air which is greatly influenced by the local terrain, i.e. the Earth's surface. For structural design purposes, it is important to understand the atmospheric boundary layer and the flow characteristics associated with it. Although wind tunnels have been extensively used to simulate such ABL in their test sections, there are many aspects of information considering the wind profile parameters that still difficult to measure. Therefore, numerical simulations represent an important additional investigative tool.

In this paper, the CFD calculation model has been established, with an aim to properly simulate the exact conditions that exist in wind tunnels during the ABL tests. CFD analyses were performed in order to validate the adopted calculation algorithm and setups for wide speed range and different terrain types. Experimental results for three test cases, from two different wind tunnels, have been used for verifications. In the first wind tunnel, small speeds were used, in the range  $1 \div 4$  m/s, while in the second tunnel, the speed of 45 m/s was applied. Depending on the obstacle types applied in wind tunnels for ABL simulations, tests in the first tunnel were divided to two cases, while in the second tunnel one test setup has been investigated.

The velocity profiles obtained by CFD analyses, using here presented calculation model, were compared with the experimental results, and good agreements have been obtained for operational engineering purposes. By this, here presented CFD calculation model can successfully be used to substitute a certain part of the expensive wind tunnel tests, both in the definition of optimum obstacle setups for ABL simulations, and for further tests of building structure models.

Another important aspect in obstacle setup verifications is proper fitting of the ABL velocity profile by log law in inner, and power law in outer domain, using indirect approach. The three experimentally obtained velocity profiles that were used for the validation of CFD calculations, were first fitted by the log law in the inner domains, and later by power law in outer domains. The two independent fitting procedures have achieved very good correlation, showing that the first experiment would correspond to ABL generated over flat and smooth terrain, second to a suburban area ABL, and third by a large city building structures. Such simple but efficient fitting procedure can be used both in wind tunnel tests and in CFD analyses in order to verify if the selected obstacle setup gives the desired type of ABL velocity profile, corresponding to the actual environment that should be simulated.

## References

- [1] Zarraonandia G 2010 *Influence on Wind Shear and Turbulence in Flow Over*, University of Norwegian, MSc Thesis
- [2] Lindgren B and Johansson A 2002 *Design and Evaluation of a low speed Wind Tunnel with Expanding Corners*, Technical report TRITA-MEK 14
- [3] Stangroom P 2004 *CFD Modelling of Wind Flow Over Terrain*, University of Nottingham, PhD Thesis
- [4] Yassen Y E and Abdelhamed A S 2015 CFD Modeling of the Atmospheric Boundary Layer in Short Test Section Wind Tunnel, *American Journal of Aerospace Engineering* **2**(1) 38-46
- [5] Yang W, Quan Y, Jin, X, Tamura Y and Gu M 2008 Influences of Equilibrium Atmosphere Boundary Layer and Turbulence Parameter on Wind Loads of Low-rise Buildings, *Journal*

- of Wind Engineering and Industrial Aerodynamics* **96**(10) 2080-2092
- [6] Karim M M, Rahman M M and Alim M A 2011 Performance of SST k- $\omega$  Turbulence Model for Computation of Viscous Drag of Axisymmetric Underwater Bodies, *IJE Transactions B: Applications* **24**(2)139-146
- [7] Al-Nehari H, Abdel-Rahman A K, Nassib A and Shafey H M 2010 Design and Construction of A Wind Tunnel for Environmental Flow Studies, *Journal of Engineering Sciences, Assiut University* **38**(1) 177-193
- [8] Stefanović Z and Pešić S 1992 *Simulation of Atmospheric Boundary Layer in Laboratory Conditions*, International Symposium on Contemporary Problems in Fluid Mechanics, Belgrade, Serbia
- [9] Wieringa J 1993 Representative Roughness Parameters for Homogeneous Terrain, *Journal of Boundary Layer Meteorology* **63** 323-363
- [10] Zaki A S, Hagishima A, Tanimoto J, Mohammad F A and Razak A A 2014 Estimation of Aerodynamic Parameters of Urban Building Arrays Using Wind Tunnel Measurements, *Journal of Engineering Science and Technology* **9**(2) 176-190
- [11] Farell C and Iyengar S K A 1999 Experiments on the Wind Tunnel Simulation of Atmospheric Boundary, *Journal of Wind Engineering and Industrial Aerodynamics* **79** 11-35
- [12] Farell C and Iyengar S K A 2001 Experimental Issues in Atmospheric Boundary Layer Simulations: Roughness Length and Integral Length Scale Determination, *Journal of Wind Engineering and Industrial Aerodynamics* **789** 1059-1080
- [13] Dutta R S 2004 *Boundary Layer Characteristics Just Above Sub-Urban Roughness*, University of Texas Tech, MSc Thesis
- [14] Holmes D J 2001 *Wind Loading of Structures*, Spon Press
- [15] Ikhwan M 2005 *Investigation of Flow and Pressure Characteristics around Pyramidal Buildings*, University of Karlsruhe, PhD Thesis
- [16] ANSYS FLUENT 16.0, *Theory Guide 2015*, ANSYS Inc
- [17] Kemmer G and Keller S 2010 Nonlinear Least- Squares Data Fitting in Excel Spreadsheets, *Article in Nature Protocol* **5**(2) 267-281